International Journal of Mechanical, Industrial and Aerospace Sciences
ISSN: 2517-9950
Vol:6, No:2, 2012

LQR Control for a Multi-MW Wind Turbine

Trung-Kien Pham, Yoonsu Nam, Hyungun Kim, Jaehoon Son

***Abstract*—**This paper addresses linear quadratic regulation (LQR) for variable speed variable pitch wind turbines. Because of the inherent nonlinearity of wind turbine, a set of operating conditions is identified and then a LQR controller is designed for each operating point. The feedback controller gains are then interpolated linearly to get control law for the entire operating region. Besides, the aerodynamic torque and effective wind speed are estimated online to get the gain-scheduling variable for implementing the controller. The potential of the method is verified through simulation with the help of MATLAB/Simulink and GH Bladed. The performance and mechanical load when using LQR are also compared with that when using PI controller.

***Keywords*—**variable speed variable pitch wind turbine, multi-MW size wind turbine, wind energy conversion system, LQR control.

I. Introduction

RECENTLY, variable speed variable pitch wind turbines (VS-VP WT)are continuously increasing their market share. This configuration is the best for multi-megawatt machines because it not only can maximize energy captured over a wide range of wind speed but also reduce mechanical fatigue by using aerodynamics control systems. In this configuration, the turbine operates with variable speed and fixed pitch if the wind speed is in below rated region (region 2) to achieve maximum aerodynamic efficiency. When the wind speed is in above rated region (region 3) the rotor is regulated at its rated speed by varying pitch angle to ensure that mechanical limitations are not exceeded. The controller should be designed intelligently to transit smoothly between two regions as well as to ensure other requirements during transition such as limiting bladed-tip noise, minimizing output power fluctuations, etc.

The thrust force acting on the rotor and torque developed by the wind turbine are nonlinear functions of wind speed, rotor speed and pitch angle. Besides, modern large-size wind turbines are usually equipped with individual pitch actuators at each blade and force/moment sensors or accelerometers on tower, nacelle as well as blades. These inputs and outputs combine with structural modes to make the machine an inherently nonlinear multi-input multi-output (MIMO) system.

T. K. Pham is with Kangwon National University, South Korea (corresponding author to provide phone: +82-33-253-0840; fax: +82-33-253-4190; e-mail: ptkien.ac@gmail.com).

Y. S. Nam is with the Kangwon National University, South Korea. (e-mail: nys@kangwon.ac.kr).

H. G. Kim is with the Kangwon National University, South Korea. (e-mail: iwisk@kangwon.ac.kr).

J. H. Son is with the Kangwon National University, South Korea.

However, most control methods applied to these multi-control-objective MIMO systems are implemented by using multiple single-input-single-output (SISO) loops [1]. The basic structure of wind turbine system is illustrated in Fig. 1. This configuration has two loops which operate independently of each other. The top part of this figure is the pitch control loop which has major role for regulating the rotor speed in the above rated region. Under a wind with the speed below the rated wind speed, the blade pitch angle is pitched off at optimal value so as to maintain max-Cp operation. Also, in this region, varying the rotor speed proportionally to the wind speed is the function of torque control loop presented in the bottom part of the figure.

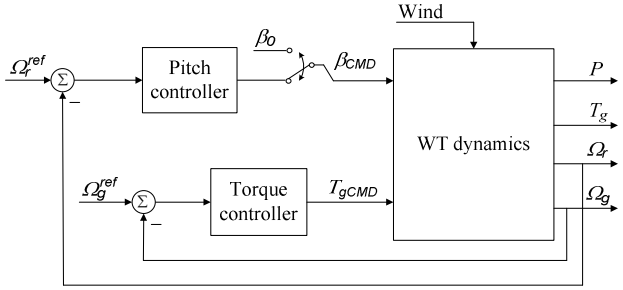

Fig. 1 Control loop of a MW Wind turbine

The linear quadratic control technique has been applied for wind turbine, such as we can find in [2], [3], [4]. Most of them focus on high wind speed region or have different control strategies for different regions. The purpose of this work is to design a MIMO LQR controller for a multi-megawatt wind turbine. The proposed controller has the same strategy for the entire operating region. The controller is synthesized with the objective of trade-off between maximizing energy captured from the wind and mitigating mechanical load. Because of the nonlinearity of the wind turbine, the controller is designed for specific operating points. The feedback gains are then interpolated or extrapolated for the whole operating region. The potential of LQR controller is verified by a commercial wind turbine simulation package GH Bladed, and compared with PI controller.

The paper is presented as follows. In section II, we present the modeling of the wind turbine: we explain the nonlinearity of the wind turbine and derive linearized model. Section III is devoted to the development of the linear quadratic optimal control which aims for trade-off among control objectives. Finally, in section IV, the proposed controller is illustrated in a high-fidelity simulation environment on a representative 2MW wind turbine.

II. WIND TURBINE MODEL

A basic block diagram for the entire variable speed variable pitch wind energy conversion system can be structured as several interconnected subsystems, shown in Fig. 2.

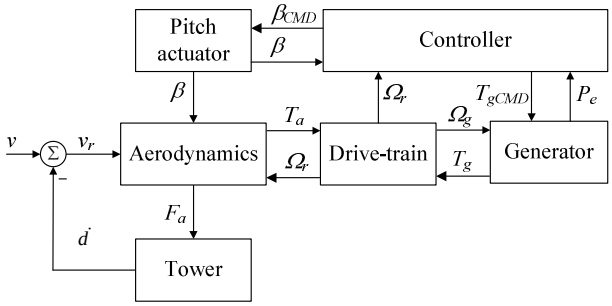

Fig. 2 A block diagram for VS-VP WT

In the above figure, F_a is thrust force. β is blade pitch angle. T_a and T_g are aerodynamic torque and reaction generator torque, respectively. Ω_r and Ω_g are rotor speed and generator speed. v is wind speed which is described by mean wind speed v_m and turbulent wind v_t, given by (1).

$$v = v_m + v_t \tag{1}$$

The wind speed v_r seen by rotor plane is defined by (2), where d is nacelle displacement.

$$v_r = v - \dot{d} \tag{2}$$

A. Aerodynamic conversion

The thrust force acting on the entire rotor, useful torque developed by the wind turbine and aerodynamic power captured from the wind are expressed by highly nonlinear equations as follow

$$F_a = \frac{1}{2}\rho\pi R^2 C_T(\lambda,\beta)v_r^2 \tag{3}$$

$$T_a = \frac{1}{2}\rho\pi R^3 \frac{C_P(\lambda,\beta)}{\lambda}v_r^2 \tag{4}$$

$$P_a = \frac{1}{2}\rho\pi R^2 C_P(\lambda,\beta)v_r^3 \tag{5}$$

Where ρ is air density, R is rotor radius. C_T is force coefficient, and C_P is called power coefficient which represents the wind turbine power conversion efficiency. C_T and C_P are functions of blade pitch angle and tip-speed ratio, λ, defined by

$$\lambda = R\Omega_r / v_r \tag{6}$$

The coefficients C_T and C_P are very important in the turbine control system design. Those characteristics for different values of tip-speed ratio and pitch angle are illustrated in Fig. 3 and Fig. 4. Fig. 3 indicates that there is one set of specific λ and β at which the turbine power coefficient is maximum, $C_P$max. It means that if the pitch angle is fixed at optimal value β_0 and varying rotor speed proportionally to wind speed to keep tip-speed ratio at λ_0, where C_P coefficient is maximum, wind turbine will extract the maximum power from the wind. However, this operation condition occurs only in low wind speed region. When wind speed is high, tip-speed ratio and pitch angle are away from their optimal values to ensure the power and rotor speed being regulated around their rated values, in order to avoid exceeding electrical power as well as mechanical stresses.

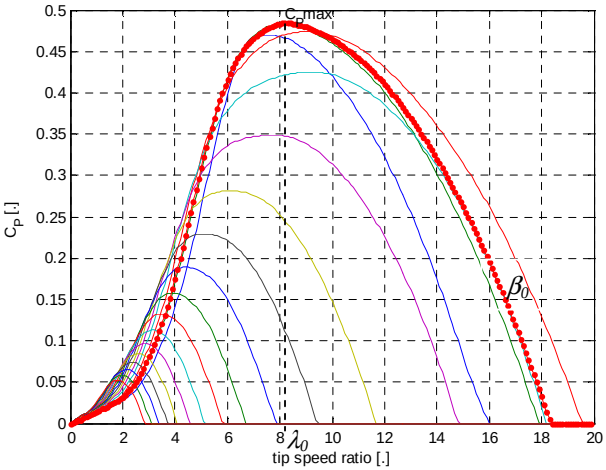

Fig. 3 Power coefficient C_P

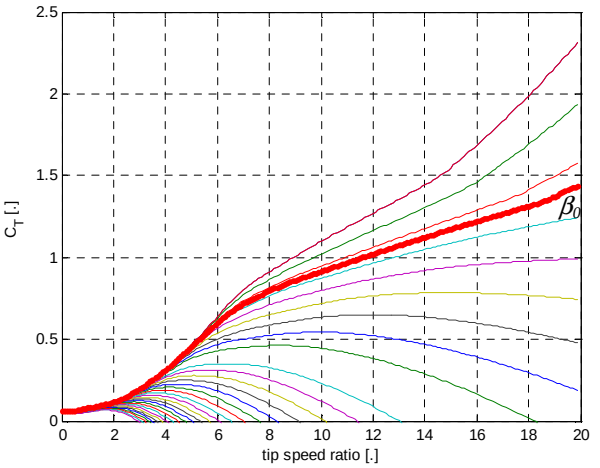

Fig. 4 Force coefficient C_T

B. Drive-train dynamics

The aerodynamic torque from equation (4) is the input of the drive-train system in low speed side. The drive-train system can be modeled as two inertias interconnected by a spring-damper and a gearbox, schematically represented in Fig. 5. On the high speed side of drive-train system the generator is mounted giving opportunity to control the reaction torque from the generator [2]. The dynamic model of the drive-train system is modeled of the form (7) and (8). Where Ω_r, Ω_g are rotor speed and generator speed, respectively. J_r, J_g are rotor inertia and generator inertia, respectively. B_r, B_g are, respectively, the damping of low speed shaft and high speed shaft. k_s and c_s are the torsional stiffness and torsional damping of drive-train axis.

$$J_r\frac{d\Omega_r}{dt} = T_a - k_s(\theta_r - \frac{1}{N}\theta_g) - c_s(\Omega_r - \frac{1}{N}\Omega_g) - B_r\Omega_r \tag{7}$$

$$J_g\frac{d\Omega_g}{dt} = \frac{k_s}{N}(\theta_r - \frac{1}{N}\theta_g) + \frac{c_s}{N}(\Omega_r - \frac{1}{N}\Omega_g) - B_g\Omega_g - T_g \tag{8}$$

The gearbox ratio N is defined as $N = \Omega_g/\Omega_r$

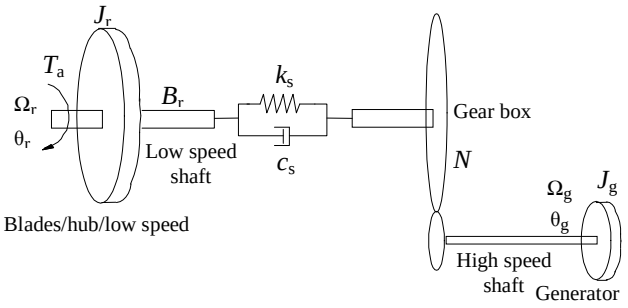

Fig. 5 A drive-train model

C. Tower dynamics

For controller design purposes, it was considered to use a sufficiently simplified axis-symmetric tower model [5]. In this work, tower top equivalent displacement of only first bending mode of fore-aft direction is considered, that is modeled by an equal common mass-spring-damper system. As a consequence, the tower top rotation, the torsion deformation, the yawing effects and higher bending modes are neglected. The first bending mode of fore-aft direction is expressed by (9).

$$M_T\ddot{d} + C_T\dot{d} + K_T d - F_a = 0 \tag{9}$$

Where M_T is the tower top effective mass, which is determined by the sum of nacelle mass including rotor and a top equivalent tower mass. C_T, K_T are, respectively, the structural damping and bending stiffness. d, $\dot{d}$ and $\ddot{d}$ are the tower top fore-aft displacement, velocity and acceleration, respectively.

D. Generator dynamics

The most common types of generators for multi-MW wind turbine are a doubly fed induction generator (DFIG) and a permanent magnet synchronous generator (PMSG) [6]. The generator torque is controlled by a power converter which also manages the active and reactive powers of the generator. High speed switching power electronics is able to set electric generator torque almost instantaneously with respect to the mechanical dynamics. For the purposes of control system design, the generator dynamics is sufficiently modeled by a first order transfer function presented in (10)

$$\frac{T_g(s)}{T_{g_{CMD}}(s)} = \frac{1}{1+\tau_g s} \tag{10}$$

In the above equation, $T_g(s)$ and $T_{gCMD}(s)$ are the generator torque and generator torque command, respectively. τ_g is the time constant of the generator dynamics.

E. Pitch actuator

While wind turbine system operates in above rated wind speed, high rotor speed that may cause mechanical damage can no longer be managed by increasing generated power because this would lead to overload the generator and converter [4]. As seen in Fig. 3, C_P can be reduced by varying the pitch angle β to maintain the output power at rated power and to regulate the rotor speed at its rated value, instead of changing rotor speed proportionally to the wind speed as in low wind speed region.

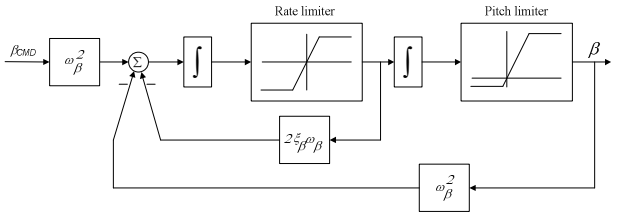

Fig. 6 A second order pitch actuator model

The pitch actuator is a nonlinear servo that generally rotates all the blades or part of them in unison. In closed loop the pitch actuator can be modeled as a linear low-order dynamic system with saturation in the amplitude and derivative of the output signal. Fig. 6 shows a block diagram of a second-order actuator model. The dynamic behavior of the pitch actuator operating in its linear region is described by following transfer function

$$\frac{\beta(s)}{\beta_{CMD}(s)} = \frac{\omega_\beta^2}{s^2 + 2\xi_\beta\omega_\beta + \omega_\beta^2} \tag{11}$$

Where β and β_{CMD} are the actual and desired pitch angle, respectively. ω_β and ξ_β are, respectively, natural frequency and damping ratio of pitch actuator dynamics. For a multi-MW wind turbine, the pitch angle ranges from -3^o to 90^o and varies at a maximum rate of $\pm 10^o$/s.

III. CONTROLLER DESIGN

A. Model for controller design

Equations from (7) to (11), describing the dynamics of wind turbine, can be written in compact form as

$$\begin{cases} f(x, \dot{x}, u, v, t) = 0 \\ y = g(x) \end{cases} \tag{12}$$

By defining the state, input and output vectors

$$x = \begin{bmatrix} d & \dot{d} & \beta & \dot{\beta} & \Omega_r & T_g \end{bmatrix}^T \tag{13}$$
$$u = \begin{bmatrix} \beta_{CMD} & T_{g_{CMD}} \end{bmatrix}^T ; y = \Omega_r$$

Equation (12) is highly nonlinear model, due to the expression of extracted thrust force F_a and aerodynamic torque T_a as in (3) and (4). In order to design controller, the global model can be linearized around operating points by linearizing the aerodynamic torque and thrust force. The deviations of aerodynamic torque and thrust force from steady state values are expressed in (14).

$$\begin{aligned} \delta T_a &= k_{\Omega_r}^{T_a}\delta\Omega_r + k_\beta^{T_a}\delta\beta + k_{v_r}^{T_a}\delta v_r \\ \delta F_a &= k_{\Omega_r}^{F_a}\delta\Omega_r + k_\beta^{F_a}\delta\beta + k_{v_r}^{F_a}\delta v_r \end{aligned} \tag{14}$$

Where the operator δ corresponds to the deviation of values from linearization point $OP(x_0, u_0, v_0)$, and coefficients in above equations are defined by

$$\begin{aligned} &k_{\Omega_r}^{T_a} = \partial T_a/\partial\Omega_r\big|_{OP} ; k_\beta^{T_a} = \partial T_a/\partial\beta\big|_{OP} ; k_{v_r}^{T_a} = \partial T_a/\partial v_r\big|_{OP} \\ &k_{\Omega_r}^{F_a} = \partial F_a/\partial\Omega_r\big|_{OP} ; k_\beta^{F_a} = \partial F_a/\partial\beta\big|_{OP} ; k_{v_r}^{F_a} = \partial F_a/\partial v_r\big|_{OP} \end{aligned} \tag{15}$$

Thus, wind parameterized linear model of wind turbine around an operating point can then be set on state space representation as in (16).

$$\begin{cases} \delta\dot{x} = A(v_0)\delta x + B(v_0)\delta u + B_v(v_0)\delta v_r \\ \delta y = C\delta x \end{cases} \quad (16)$$

Where $\delta x = x - x_0; \delta u = u - u_0; \delta y = y - y_0$

State space matrices $A(v_0)$, $B(v_0)$ and $B_v(v_0)$ depend on operating points.

$$A(v_0) = \partial f / \partial x \Big|_{OP}; B(v_0) = \partial f / \partial u \Big|_{OP}; B_v(v_0) = \partial f / \partial v_r \Big|_{OP} \quad (17)$$

$C = [0 \quad 0 \quad 0 \quad 0 \quad 1 \quad 0]$

The controller which is designed base on linear system expressed in equation (18) often proves unsatisfactory in controlling the turbine to the desired rotor rotational speed. This may be due to some linearization inaccuracies or some model deficiencies with respect to the machine behavior in real operating conditions. Keeping the rotor speed to a preset value is usually of paramount importance, so it may be useful to add a complimentary term to the formulation in order to represent a long term deviation of the actual rotational speed with respect to the set point. The linearized wind turbine expressed in (16) is augmented with rotor speed integrator. This gives the state vector of the linear system with the form as in (18).

$$\delta x = \left[\delta d \quad \delta\dot{d} \quad \delta\beta \quad \delta\dot{\beta} \quad \delta\Omega_r \quad \delta T_g \quad \int_{t_o}^{t_f} \delta\Omega_r dt \right]^T \quad (18)$$

Thus, the state space model of augmented system is described as

$$\begin{cases} \delta\dot{x} = \begin{bmatrix} A(v_0) & \Theta_1 \\ C & 0 \end{bmatrix}\delta x + \begin{bmatrix} B(v_0) \\ \Theta_2 \end{bmatrix}\delta u + \begin{bmatrix} B_v(v_0) \\ 0 \end{bmatrix}\delta v_r \\ \delta y = [C \quad 0]\delta x \end{cases} \quad (19)$$

Where $\Theta_1 = [0 \ 0 \ 0 \ 0 \ 0 \ 0]^T$; $\Theta_2 = [0 \ 0]$

B. Target trajectory

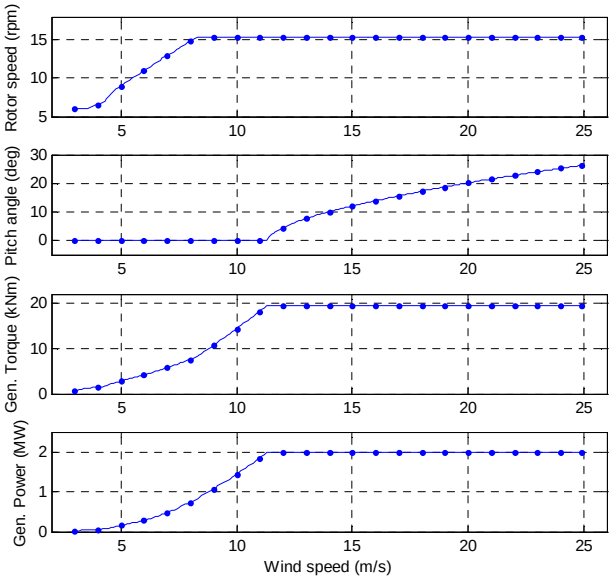

Fig. 7 Schedule for regulation set point

As mention above, when wind speed is in below rated region, the blade pitch angle is constantly maintained at optimal value β_0. While the rotor speed is changed proportional to wind speed so as to maintain tip speed ratio at constant value λ_0. For above rated region, the pitch angle is varied in order to regulate the rotor speed and generator torque/power at rated values. Fig. 7 illustrates the goal trajectories for rotor speed (the first window), blade pitch angle (the second window), generator torque (the third window) and electrical power (the fourth window).

C. LQR design

With the operating points determined, a set of controllers can be synthesized by applying LQR for augmented model presented in (19), with a quadratic cost function for the regulation problem at an operating point is defined as

$$J = \int_0^\infty \left(\delta x^T Q(v_0)\delta x + \delta u^T R(v_0)\delta u \right) dt \quad (20)$$

Where $Q(v_0)$ and $R(v_0)$ are nonnegative and symmetric matrices of weights. The control law optimizing the above criterion J is a state feedback law with an optimal gain matrix $K(v_0)$ determined by solving an LQR problem. In the implementation, the intermediate controllers are then interpolated linearly from the discrete number of controllers which have been designed for specific operating points. Fig. 8 illustrates the structure of wind turbine system. The LQR gains are scheduled by effective wind speed, estimated by wind speed estimator. This estimation will be presented in the following subsection.

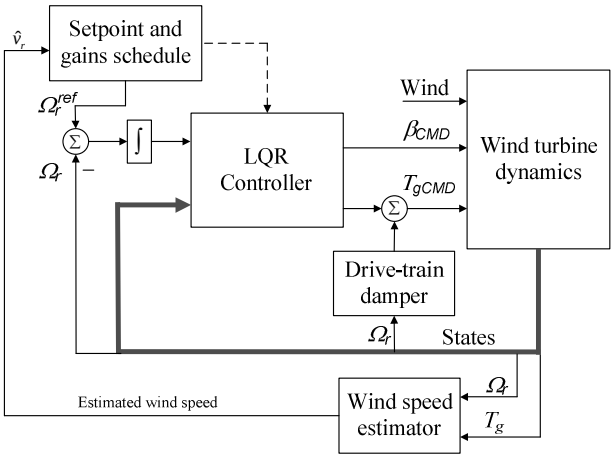

Fig. 8 LQR control system

IV. Wind Speed Estimation

As explained above, the target trajectories are scheduled by wind speed. However, there is a very rough measurement of the wind speed available. It is therefore necessary to have a good wind speed estimator to get the controllers implementable. Fig. 9 shows the schematic diagram of the wind speed estimator, which consists of two consecutive processing modules. The first module is the aerodynamic torque estimation, following by 3-D lookup table to calculate the effective wind speed.

The governing equations of the drive-train model (7) and (8) can be combined into one equation of

$$J_t \frac{d\Omega_r}{dt} = T_a - NT_g - T_L \quad (21)$$

Where $J_t = J_r + N^2 J_g$, and T_L represents all the mechanical

losses.

Then, augmenting (21) with the unknown aerodynamic torque T_a, the above equation can be expressed in the state space form of (22) [6], [7].

$$\dot{x} = \begin{Bmatrix} \dot{\Omega}_r \\ \dot{T}_a \end{Bmatrix} = \begin{bmatrix} 0 & 1/J_t \\ 0 & 0 \end{bmatrix} \begin{Bmatrix} \Omega_r \\ T_a \end{Bmatrix} + \begin{pmatrix} -N/J_t \\ 0 \end{pmatrix} T_g + \begin{pmatrix} -1/J_t \\ 0 \end{pmatrix} T_L + \begin{pmatrix} -N/J_t \\ N \end{pmatrix} w_g \quad (22)$$

$$y = \begin{bmatrix} 1 & 0 \end{bmatrix} \begin{Bmatrix} \Omega_r \\ T_a \end{Bmatrix} + w_v$$

where w_g and w_v represent the input process and output sensor noise. A Kalman filter is applied to estimate the aerodynamic torque, which has the structure of (23). In which, variables with hat are to be estimated and L is the Kalman filter gain .

$$\dot{\hat{x}} = \begin{Bmatrix} \dot{\hat{\Omega}}_r \\ \dot{\hat{T}}_a \end{Bmatrix} = \begin{bmatrix} 0 & 1/J_t \\ 0 & 0 \end{bmatrix} \begin{Bmatrix} \hat{\Omega}_r \\ \hat{T}_a \end{Bmatrix} + \begin{pmatrix} -N/J_t \\ 0 \end{pmatrix} T_g + \begin{pmatrix} -1/J_t \\ 0 \end{pmatrix} T_L + L\left(\Omega_r - \hat{\Omega}_r\right) \quad (23)$$

The second stage of wind speed estimation is to calculate wind speed through a 3-D lookup table, which has three inputs of estimated aerodynamic torque, measured rotor speed and measured pitch angle. This 3-D lookup table is build by using equation (4), which is reformulated in the form of.

$$\hat{T}_a = \frac{1}{2}\rho\pi R^3 \left\{ \frac{C_P\left(\hat{\lambda}, \beta\right)}{\hat{\lambda}} \right\} \hat{v}_r^2 \quad (24)$$

where $\hat{\lambda}(= R\Omega_r / \hat{v})$ is estimated tip-speed ratio.

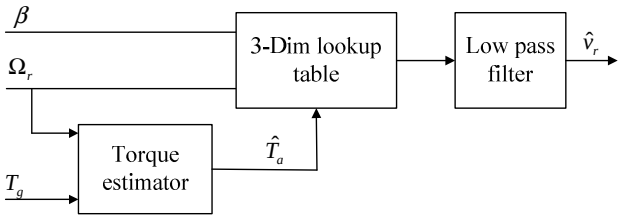

Fig. 9 Wind speed estimator

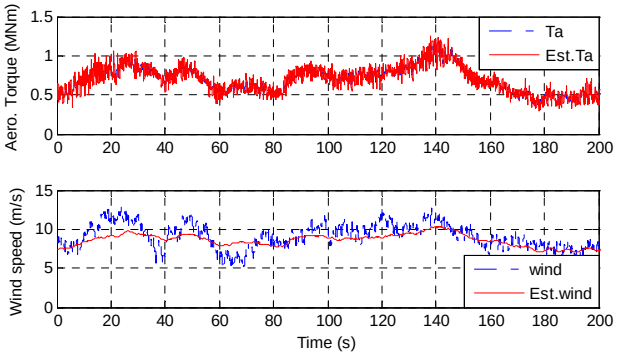

Fig. 10 Estimated aerodynamic torque (above) and estimated wind speed (below)

Fig. 10 illustrates the estimated aerodynamic torque and estimated wind speed with the mean value of 8m/s and 23% TI. The real signals are presented in dash-dot and the estimated values in solid lines. It is noticed that the solid line in bottom window of Fig. 10 is spatially average wind speed, which is a little difference from the wind speed measured at the hub (dash-dot line). The high frequency components in the turbulent wind are filtered out so as to get estimated wind as a good scheduling variable.

V. Numerical Simulation

The proposed controller is validated through simulations with stochastic wind input in both two regions. The performance and mechanical load of proposed method are compared with that of PI controller. The control law is developed in MATLAB/Simulink and compiled into a Dynamic Link Library (DLL). The external controller in DLL format will be used with GH Bladed package to perform full system simulation of wind turbine.

The simulation for below rated region is performed using a wind with mean speed of 8m/s, which is perturbed by turbulent wind with turbulence intensity of 23%. The trace of hub height wind speed is shown in the top window of Fig. 11. Fig. 11 also shows the rotor speed behavior, generator torque, generator power and tower fore-aft moment versus time. The solid plots of Fig. 11 represent the responses of the wind turbine when using PI controller (designed in [6]), while the dash-dot lines are the wind turbine responses when using LQR controller. The difference of performance responses between two controllers are summarized in Table I. It is difficult to differentiable between the structural responses such as blade or tower bending moment in time domain. The damage equivalent loads (DEL), M_{eq}, can be a quantitative measure. M_{eq} is given by (25)

$$M_{eq} = \sqrt[m]{\frac{\sum_k \left(M_k\right)^m n_k}{n_{tot}}} \quad (25)$$

where n_k is the number of cycles in mechanical load range M_k and n_{tot} is the total number of cycles in a mechanical load signal. m is the material specific number, for example m = 3.5 for a steel tower structure and m = 10 for a fiber glass blade [8]. The larger the DEL value is, the more prone to end up in fatigue failure. The statistical data of DEL data of structural load responses at mean wind speed of 8m/s for both LQR and PI controller are summarized and compared in Table II. The performance data shows that when using LQR the mean value of electrical power slightly decreases, however the DEL of the

TABLE I
Performance data at wind speed of 8m/s 23%TI

Performance data	Rotor speed (rpm)		Generator Power (Mw)	
	Mean	Std.	Mean	Std.
PI (A)	13.999	1.42	0.778	0.252
LQR (B)	14.165	1.43	0.777	0.247
(B-A)/A (%)	1.18	0.70	-0.13	-1.98

TABLE II
Mechanical load at wind speed of 8m/s 23%TI

DEL	Blade moment (kNm)		Tower fore-aft moment (kNm)
	In plane	Out-of plane	
PI (A)	2107	1618	4298
LQR (B)	2061	1535	4030
(B-A)/A (%)	-2.18	-5.13	-6.23

blade bending moment in the in-plane and the out-of-plane direction as well as the tower root bending moment in the fore-aft direction are improved.

Fig. 12 shows the time domain response simulation for above rated wind speed region. The wind speed in this simulation has the mean value of 18m/s with turbulence intensity of 16%. The first window of Fig. 12 shows the wind speed measured at the hub. The second one shows the rotor speed. The next windows present generator torque, generator power and blade pitch angle. It is easy to see that, in high wind speed region, LQR's performance is quite good when comparing with PI. It can be seen in Table III, the electrical power slightly increases. It also shows that there are remarkable improvements in the fluctuations of rotor speed and electrical power around rated values. These are proved by standard deviations of rotor speed and electrical power in Table III. Furthermore, there is more than 20% DEL decrease of the tower bending moment in fore-aft direction, as shown in Table IV.

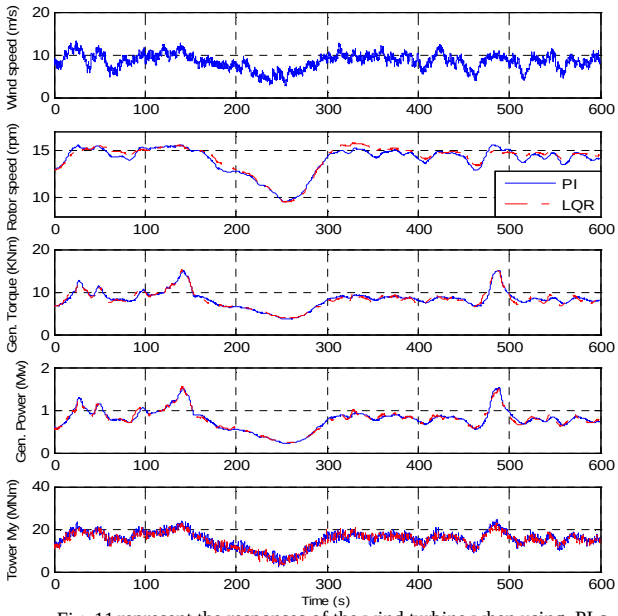

Fig. 11 represent the responses of the wind turbine when using PI c ontroller designed in [6])

TABLE III
PERFORMANCE DATA AT WIND SPEED OF 18M/S 16%TI

Performance data	Rotor speed (rpm)		Generator Power (Mw)	
	Mean	Std.	Mean	Std.
PI (A)	15.270	0.3317	1.9873	0.0513
LQR (B)	15.299	0.1785	1.9916	0.0300
(B-A)/A (%)	0.19	-46.18	0.21	-41.52

VI. CONCLUSION

This paper investigated in designing a wind-scheduling linear quadratic controller with online wind speed estimation for a multi-MW size wind turbine. The controller was designed by linearising the nonlinear wind turbine along the operating point trajectory. The potential of the controller was checked by simulating with GH Bladed software. The responses of proposed method were compared with that of PI controller.

TABLE IV
MECHANICAL LOAD AT WIND SPEED OF 18M/S 16%TI

DEL	Blade moment (kNm)		Tower fore-aft moment (kNm)
	In plane	Out-of plane	
PI (A)	2386	2472	7268
LQR (B)	2367	2502	5808
(B-A)/A (%)	-0.79	1.21	-20.09

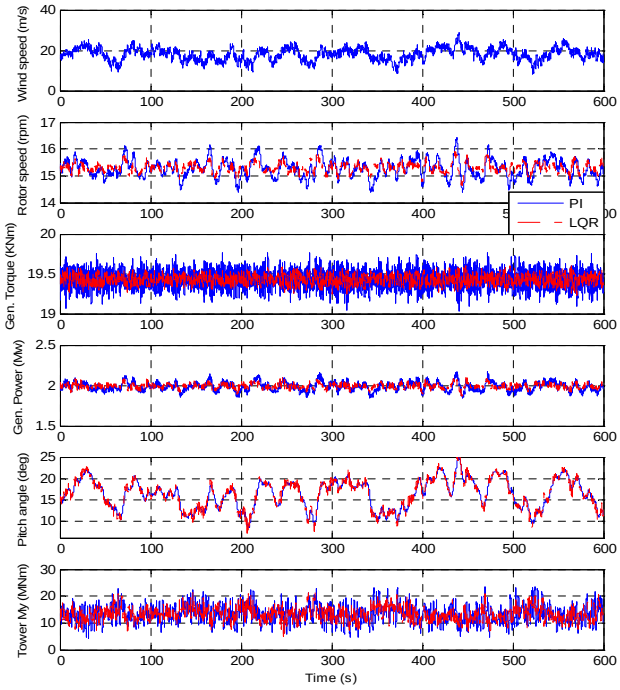

Fig. 12 Simulation result for wind speed of 18m/s 16% TI

ACKNOWLEDGEMENT

This work was supported by the New & Renewable Energy of the Korea Institute of Energy Technology Evaluation and Planning (KETEP) grant funded by the Korea government Ministry of Knowledge Economy (No. 20103010020040)

REFERENCES

[1] E.A. Bossanyi, "The design of closed loop controllers for wind turbines", *Wind energy*, vol. 3, 2000, pp. 148-163.

[2] K.Z. Ostergaard, P. Brath, J. Stoustrup, "Gain-scheduling linear quadratic control of wind turbines operating at high wind speed", *16th IEEE International Conference on Control Applications*, Singapore, 2007, pp. 276-281.

[3] K. Stol, m. Balas, "Full-state feedback control of a variable-Speed wind turbine: A comparison of periodic and constant gains", *ASME J. Solar energy engineering*, vol.123(4), 2001, pp. 319-326.

[4] E.B. Muhando, T. Senjyu, H. Kinjo, T. Funabashi, "Augmented LQG controller for enhancement of online dynamic performance for WTG system", *Renewable energy*, vol. 33, 2008, pp. 1942-1952.

[5] E. L. van der Hooft, P. Shaak, T.G. van Engelen, "Wind turbine control algorithms," ECN-C-03-111, 2003.

[6] Y. Nam, J. Kim, I. Paek, Y.H. Moon, S.J. Kim, D.J. Kim, "Feedforward Pitch control using wind speed estimation", *Journal of Power Electronics*, Vol. 11, No. 2, 2011, pp. 211-217.

[7] K.Z. Ostergaard, P. Brath, J. Stroustrup, "Estimation of effective wind speed", *Journal of Physics: Conference Series*, vol. 75, 2007, pp. 1-9.

[8] E.A. Bossanyi, "GH Bladed theory manual (version 3.81)", Garrad Hassan and Partners, 282-BR-009, 2008